

## Article

# Beam-Plasma Stabilizer for the New Type of Nuclear Power Energy Systems

Alexander Mustafaev <sup>1</sup>, Artem Grabovskiy <sup>1</sup>, Alexander Krizhanovich <sup>1,\*</sup>  and Vladimir Sukhomlinov <sup>2</sup>

<sup>1</sup> The Department of General & Technical Physics, Saint Petersburg Mining University, 199106 Saint Petersburg, Russia; Mustafaev\_AS@pers.spmi.ru (A.M.); Grabovskiy\_AYu@pers.spmi.ru (A.G.)

<sup>2</sup> The Department of Optics, Saint Petersburg State University, 199034 Saint Petersburg, Russia; v\_sukhomlinov@mail.ru

\* Correspondence: sanek.9510@yandex.ru

**Abstract:** In this paper the electrokinetic characteristics of helium low-voltage beam discharge plasma in operating conditions of a three-electrode device with a hot cathode are studied. A method and a device are proposed to ensure effective voltage stabilization in a range up to 110 V by controlling the electron velocity distribution function using the plasma channel external boundaries.

**Keywords:** anisotropic plasma; hot cathode; beam discharge; voltage stabilization; plasma channel; electron velocity distribution function (EVDF); current-voltage curve; plasma energetics; three-electrode device



**Citation:** Mustafaev, A.; Grabovskiy, A.; Krizhanovich, A.; Sukhomlinov, V. Beam-Plasma Stabilizer for the New Type of Nuclear Power Energy Systems. *Appl. Sci.* **2021**, *11*, 11419. <https://doi.org/10.3390/app112311419>

Academic Editor: Xinpei Lu

Received: 31 October 2021

Accepted: 30 November 2021

Published: 2 December 2021

**Publisher's Note:** MDPI stays neutral with regard to jurisdictional claims in published maps and institutional affiliations.



**Copyright:** © 2021 by the authors. Licensee MDPI, Basel, Switzerland. This article is an open access article distributed under the terms and conditions of the Creative Commons Attribution (CC BY) license (<https://creativecommons.org/licenses/by/4.0/>).

## 1. Introduction

One of the most important anisotropic plasma applications is plasma energetics [1,2]. The development of space nuclear power plants (NPP) started in the beginning of the 1960s, and by the end of the 1980, the Buk [3] and Topaz [4] nuclear power plants were created, tested, and proved to be successful in terms of their orbital operation, providing energy a whole series of spacecraft.

Today, compact and highly efficient nuclear power plants have been developed [5,6]. Such installations have already made it possible to solve the problems of power supply for industrial facilities and social infrastructure in hard-to-reach regions around the world, where the use of imported hydrocarbon fuel greatly increases the price of electricity and heat.

For the effective operation of such nuclear power plants, a wide range of reliable electronic devices including, but not limited to, current and voltage stabilizers, generators, rectifiers, and key elements that are capable of operating at temperatures above 1000 K and high radiation levels are required. This problem cannot be solved by traditional semiconductor devices [7]; only gas discharge devices satisfy these requirements.

The devices that are based on nonequilibrium plasma of low-voltage beam discharges (LVBD) [8–10], in which the nonlocal nature of the distribution function of charged particles allows one to control groups of electrons of different energies and thereby influence the energy characteristics of the gas-discharge devices [11,12] are of particular interest.

In this study, a new method of high-voltage stabilizing and a triode that is based on a helium LVBD special design are proposed.

## 2. Materials and Methods

The experimental set-up was thoroughly described in paper [10], so let us consider only its main elements, presented in Figure 1. Block I included a vacuum chamber (1), cathode (2), and anode (3) units. Special sapphire windows (4) were used for observation and optical measurement purposes. The vacuum system (block II) included a turbomolecular

pump that allowed one to achieve the maximum vacuum level of  $5 \times 10^{-8}$  Torr. High stability of the discharge conditions were achieved via the implementation of a long degassing cycle at the temperature of 700 K. The optical unit III consisted of the monochromator (7), the diaphragm (8), condenser lens (9), and a data processing system (10).

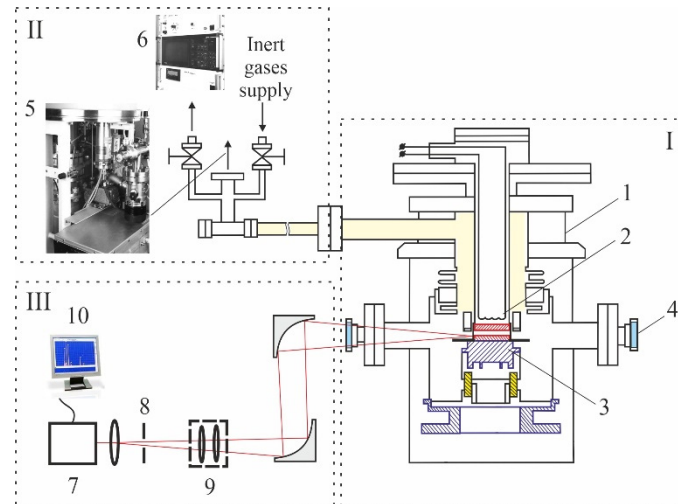


**Figure 1.** Principal layout of the experimental set-up: vacuum chamber unit (I), vacuum system (II), optical system (III), vacuum chamber (1), cathode unit (2), anode unit (3), sapphire window (4), turbomolecular pump (5), mass-spectrometry analysis system (6), monochromator (7), diaphragm (8), condenser lens (9), and experimental data processing system (10).

The device flowchart is shown in Figure 2. A thermionic cathode (1) that was impregnated with barium had a diameter of 10 mm, the molybdenum main anode (2) was fabricated in the form of a diaphragm with a diameter of 30 mm and a 2 mm central hole. The main anode (MA), located within 8 mm from the cathode, was parallel and coaxial to it. The control molybdenum electrode (CE) (3) with a diameter of 30 mm was removed from the zone of the main discharge behind the MA and was located at a distance of 1 mm from it.

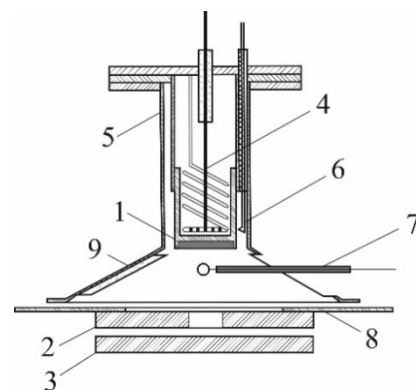


**Figure 2.** Flowchart of the device with discharge channel narrowing: cathode (1), main anode (2), external control electrode (3), heater (4), heat shield (5), cathode micro thermocouple (6), probe (7), protection aluminum insulators (8), and lateral conductive shield (9).

The main discharge gap geometry-shaping unit was adjacent to the cathode and had the form of a metal conical shield (9). The interelectrode gap was filled with spectrally pure helium. The potential of the conical shield coincided with the potential of the cathode.

The process of plasma diagnostics was carried out according to the method of the flat one-sided probe that was developed in [13]. The method is based on measuring the probe current second derivative with respect to the probe potential values and the subsequent calculation of the complete EVDF, which is represented as a series in Legendre

polynomials. During the probe measurements, all of the Langmuir's theory requirements were meticulously met. For this purpose, probes with a thickness of 30  $\mu\text{m}$  and a diameter of 0.5 mm were acquired.

To obtain the values of the probe current second derivative, we used the demodulation method that was implemented in a PC-based measuring complex. A 100% modulated voltage  $\Delta U = U_0(1 + \cos\omega_1 t)\cos\omega_2 t$  was used as a differentiating signal to increase the sensitivity of the method.

To ensure that the device entered its operating mode, one had to perform several steps. Firstly, a discharge had to be ignited at the main anode. Then a discharge had to be ignited on the control electrode, after which a fixed value of the current had to be set at the control electrode, and the corresponding volt-ampere curve had to be recorded. In this case, in the cathode-anode gap, a diffuse luminescence characteristic of the LVBD can be observed.

### 3. Results

It is well known [10] that the EVDF structure is formed by two separate groups of electrons—thermal and beam electrons. The velocity distribution of thermal electrons is close to the isotropic Maxwellian one, while the corresponding characteristic for the beam electrons is characterized by a significant distribution anisotropy. Comparison of the thermal and beam electron's energies revealed a strong nonequilibrium of the EVDF—the mean energy values for the thermal and beam electrons were about 2 eV and 25 eV, respectively. The formation of such a EVDF structure is associated with the potential distribution over the interelectrode gap (Figure 3). The curves 1–3 in Figure 3 were recorded at different helium pressures and currents on MA and CE.

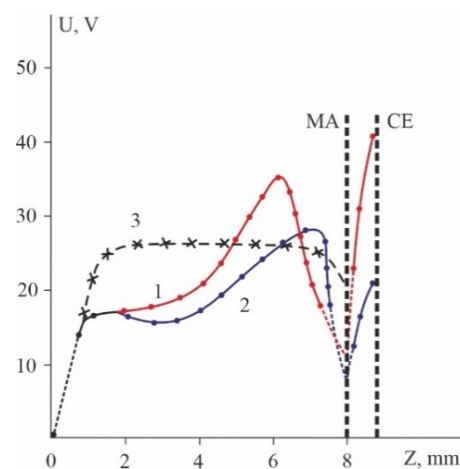


**Figure 3.** Potential distribution over the gap of the experimental device at different helium pressure values  $P_{\text{He}}$ , Torr: 1–3; 2–6; 3–2; currents to the MA, A: 1–0.6; 2–0.4; 3–0.2; currents at the CE, A: 1–0.04; 2–0.02; 3–0.

It can be seen that for zero current values at CE (curve 3) the potential distribution is typical for LVBD, and a potential drop was formed at the anode which is an almost insurmountable barrier for thermal plasma electrons, which, in this mode, do not participate in the processes of ionization and current transport. The electrons that were emitted by the cathode were accelerated in the near-cathode sheath and form a beam with a narrow energy distribution that penetrates the interelectrode gap. The creation of thermal electrons occurs as a result of the ionization of helium atoms by the beam electrons.

When the current at CE is nonzero, the potential distribution changes drastically—a potential jump is formed near the anode hole (Figure 3, curves 1, 2). Such an effect leads to the acceleration of thermal electrons to the energies that allow them to pass into the gap between MA and CE. In this case, the magnitude of the jump grows with increasing current at CE, which leads to a rise in the anisotropy of the thermal electrons' velocity distribution function.

Based on the data of probe measurements, the complete EVDF was reconstructed and its angular structure was analyzed. Figure 4 comprises of the diagrams that illustrate the angular structure of thermal plasma electrons' distribution function near the anode hole as a function of helium pressure and the current at the CE. It can be seen from Figure 4a, that a pressure increase leads to the isotropization of EVDF under the influence of elastic electron-atom collisions. Figure 4b shows an increase in the degree of thermal electrons' anisotropy due to the aforementioned acceleration effect at the potential jump near the anode hole, the value of which grows with increasing current at CE (see Figure 3).

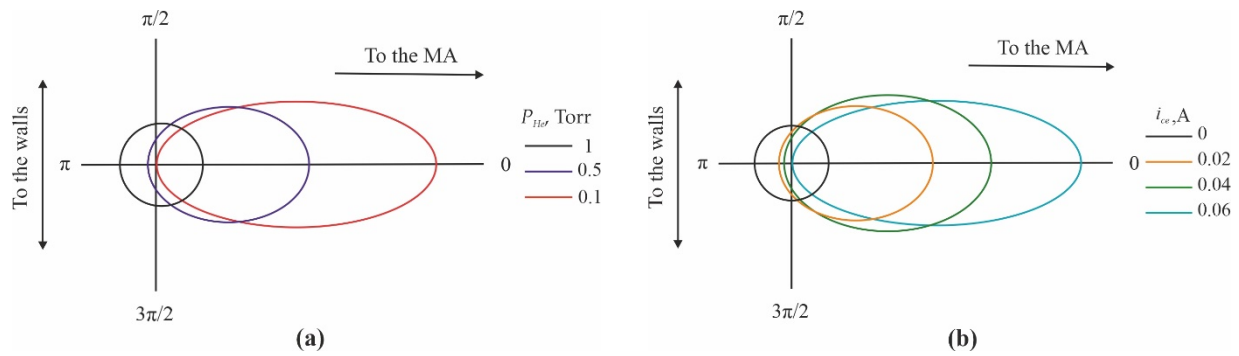


**Figure 4.** Angular structure of thermal electrons' velocity distribution function near the anode hole: (a) For different values of helium pressure; (b) For various currents at the CE  $i_{ce}$  and fixed pressure  $P_{He} = 0.5$  Torr. The horizontal axis coincides with the discharge symmetry axis.

Thus, thermal electrons begin to participate in the processes of current transport. In the gap between the MA and the CE, the current transfer is carried out mainly by thermal electrons from the plasma in the cathode-anode gap, and the hole in the anode is essentially a plasma cathode.

The current-voltage curves (registered in these modes) of the cathode—main anode (1–3) and the cathode—control electrode (4–7) gaps are presented in Figure 5. One can easily see that the curves 4–7 demonstrate significantly higher discharge voltage values compared to the curves 1–3 and thus follow the requirements of voltage stabilization in the high-voltage range.

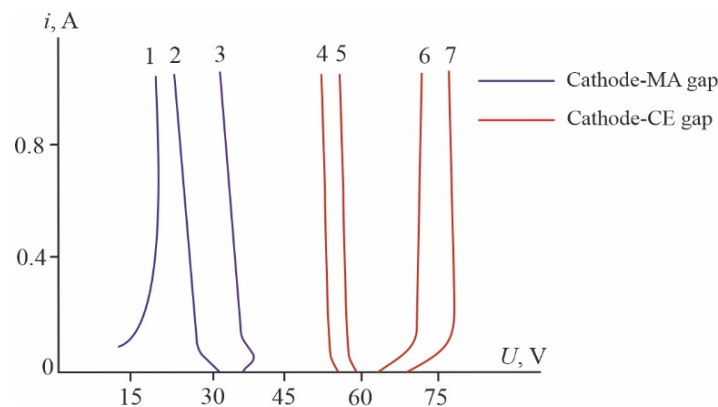


**Figure 5.** Current-voltage curves of the different gaps, registered at different helium pressure values  $P_{He}$ , Torr: 1–0.9; 2–0.3; 3–0.1; 4–1; 5–0.8; 6–0.6; 7–0.5.

#### 4. Discussion

In the considered conditions, the problem of high voltage stabilizing is solved by creating LVBD directly between the cathode and the control electrode through the main anode hole as well as via the involvement of thermal electrons in the processes of current transport. The process of stabilized voltage control can be performed in two ways. The first

method includes changing the helium pressure. With its decrease, the discharge voltage grows and reaches the values of  $U_{stab} \approx 110$  V at  $P_{He} = 0.1$  Torr (Figure 6a).

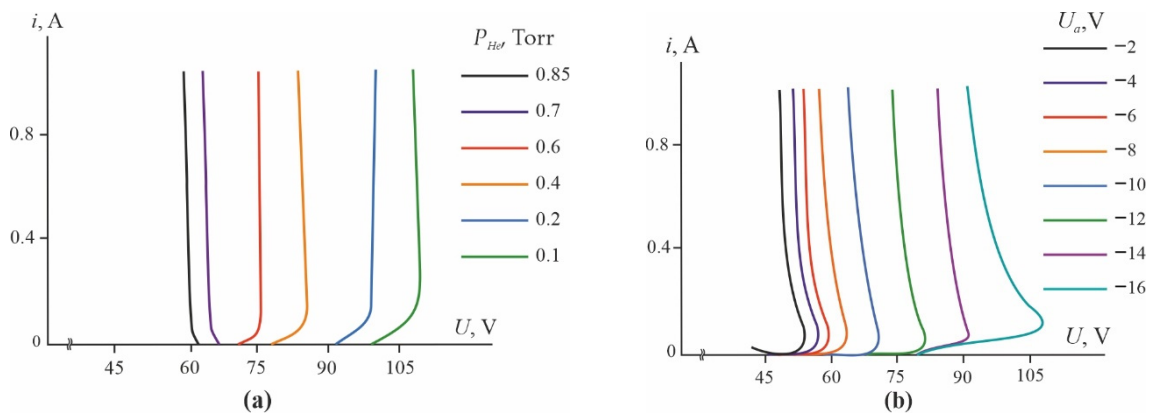


**Figure 6.** Current-voltage curves of the cathode—control electrode gap: (a) For different values of helium pressure; (b) For various negative potentials of the main anode  $U_a$  and fixed pressure  $P_{He} = 0.5$  Torr.

Another possibility requires changing the negative potential of the main anode  $U_a$  in the range between 2 and 14 V. This solves the problem of controlling the voltages up to  $U_{stab} = 90$  V (Figure 6b). A further increase in the negative potential results in the deterioration of stabilization quality (the curve at  $-16$  V, Figure 6b). The distortion of the I-V characteristic at large negative MA potentials is apparently associated with an imbalance in the processes of generation and the escape of charged particles from the plasma. To confirm this hypothesis, further research is required.

The effectiveness of the proposed plasma stabilizer is illustrated by the stabilized voltage dependence on helium pressure (Figure 7a) and on the negative potential of the main anode (for three helium pressure values (Figure 7b)).

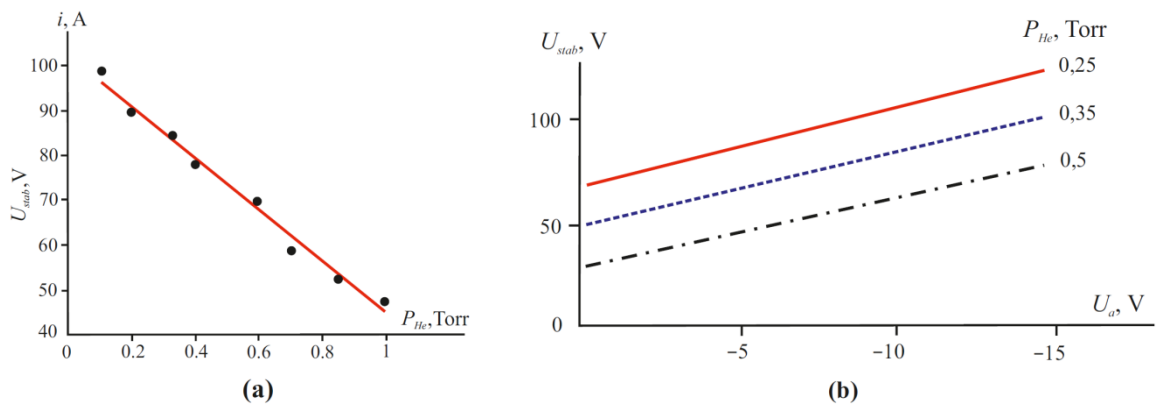


**Figure 7.** Dependence of the stabilized voltage: (a) On helium pressure  $P_{He}$ ; (b) On the negative potential of the main anode  $U_a$ .

In all cases of a decrease in energy (and, accordingly, the degree of anisotropy) of thermal electrons that is caused by an increase in the helium pressure or a decrease in the current values at CE, the possibilities of voltage stabilization deteriorate, which is confirmed by the data that is presented in Figures 5–7.

Further investigation of the EVDF formation process mechanisms near the narrowing of the discharge channel (i.e., the anode hole) and their influence on the energy characteristics of plasma devices require an extensive theoretical analysis at the kinetic level.

### 5. Conclusions

The proposed device and methods provide the means for voltage stabilization in a range between 10 V and 100 V by creating a discharge between the cathode and the control

electrode through the hole in the main anode. The control of the stabilized voltage values can be carried out both by adjusting the pressure of helium and by changing the negative potential of the main anode.

**Author Contributions:** Conceptualization, methodology, V.S.; formal analysis, investigation, A.G.; writing—original draft preparation, writing—review and editing, visualization, A.K.; data curation, writing—review and editing, supervision, project administration, A.M. All authors have read and agreed to the published version of the manuscript.

**Funding:** The research was performed at the expense of the subsidy for the state assignment in the field of scientific activity for 2021 No FSRW-2020-0014.

**Institutional Review Board Statement:** Not applicable.

**Informed Consent Statement:** Not applicable.

**Data Availability Statement:** The data presented in this study are available in the article. Initial experimental data are available on request from the corresponding author.

**Conflicts of Interest:** The authors declare no conflict of interest.

## References

1. Gupta, J.; Singla, M.K.; Nijhawan, P. Magnetohydrodynamic system—A need for a sustainable power generation source. *Magnetohydrodynamics* **2021**, *57*, 251–272. [[CrossRef](#)]
2. Boozer, A.H. Plasma steering to avoid disruptions in ITER and tokamak power plants. *Nucl. Fus.* **2021**, *61*, 054004. [[CrossRef](#)]
3. Gryaznov, G.M. *Space Nuclear Energy and New Technologies (Notes of the Director)*; FSUE “TsNIIAtominform”: Moscow, Russia, 2007; 136p.
4. Kukharkin, N.E.; Ponomarev-Stepnoy, N.N.; Usov, V.A. *Space Nuclear Power (Nuclear Reactors with Thermoelectric and Thermionic Conversion—“Romashka” and “Yenisei”)*; Ponomarev-Stepnoy, N.N., Ed.; Izdat: Moscow, Russia, 2012; 146p. Available online: <http://connections-qj.org/article/space-nuclear-power-nuclear-reactors-thermo-electric-and-thermionic-conversion-romashka-and> (accessed on 25 November 2021).
5. Ivanov, S.V.; Kuznetsov, V.I. Development of energy strategy for the Arctic and regions of the Russian Federation Far North until 2030. In Proceedings of the VI International Conference Arctic 2021, Moscow, Russia, 3–4 March 2021; pp. 10–13.
6. Krotov, A.D.; Lazarenko, G.E.; Ovcharenko, M.K.; Pyshko, A.P.; Sonko, A.V.; Yarygin, V.I.; Lazarenko, D.G. Autonomous thermal emission nuclear power plant for offshore gas and oil platforms. *Izvestiya Vuzov. Yad. Energ.* **2011**, *3*, 21–27.
7. Jiménez Carrizosa, M.; Stankovic, N.; Vannier, J.-C.; Shklyarskiy, Y.E.; Bardanov, A.I. Multi-terminal dc grid overall control with modular multilevel converters. *J. Min. Inst.* **2020**, *243*, 357–370. [[CrossRef](#)]
8. Denisov, V.V.; Akhmadeev, Y.H.; Koval, N.N.; Kovalsky, S.S.; Lopatin, I.V.; Ostroverkhov, E.V.; Schanin, P.M. The source of volume beam-plasma formations based on a high-current non-self-sustained glow discharge with a large hollow cathode. *Phys. Plasmas* **2019**, *26*, 123510. [[CrossRef](#)]
9. Adams, S.F.; Demidov, V.I.; Bogdanov, E.A.; Koepke, M.E.; Kudryavtsev, A.A.; Kurylanskaya, I.P. Control of plasma properties in a short direct-current glow discharge with active boundaries. *Phys. Plasmas* **2016**, *23*, 024501. [[CrossRef](#)]
10. Mustafaev, A.S.; Grabovskiy, A.Y. Low-voltage beam discharge in light inert gases to solve problems of voltage stabilization. *High Temp.* **2017**, *55*, 24–30. [[CrossRef](#)]
11. Korotkov, S.V.; Zhmodikov, A.L. A High-Power Diode-Dynistor Generator for Gas-Discharge Technologies. *Instrum. Exp. Tech.* **2021**, *64*, 683–686. [[CrossRef](#)]
12. Zhong, S.; Qin, F.; Gao, Y.; Yan, Z. Response Characteristics of Gas Discharge Tube to High-Power Microwave. *IEEE Access* **2021**, *9*, 111486–111492. [[CrossRef](#)]
13. Mustafaev, A.S. Probe Method for Investigation of Anisotropic EVDF. Electron Kinetics and Applications of Glow Discharges. In *NATO International Scientific Session*; Kortshagen, U., Tsendin, L., Eds.; Plenum: New York, NY, USA, 1998; Volume 367, p. 531.